



Small Things Matter: The 11.6-kDa TraB Protein is Crucial for Antibiotic Resistance Transfer Among Enterococci

Tamara M.I. Berger^{1†}, Claudia Michaelis^{2†}, Ines Probst³, Theo Sagmeister¹, Lukas Petrowitsch¹, Sandra Puchner², Tea Pavkov-Keller^{1,4,5}, Bernd Gesslbauer⁶, Elisabeth Grohmann^{2*} and Walter Keller^{1,4,5*}

OPEN ACCESS

Edited by:

Manuel Espinosa,
Margarita Salas Center for Biological
Research (CSIC), Spain

Reviewed by:

Gabriel Moncalian,
University of Cantabria, Spain
Radoslaw Pluta,
Institute for Research in Biomedicine,
Spain
Guenther Muth,
University of Tübingen, Germany

*Correspondence:

Walter Keller
walter.keller@uni-graz.at
Elisabeth Grohmann
egrohmann@bht-berlin.de

[†]These authors have contributed
equally to this work and share first
authorship

Specialty section:

This article was submitted to
Molecular Recognition,
a section of the journal
Frontiers in Molecular Biosciences

Received: 31 January 2022

Accepted: 14 March 2022

Published: 25 April 2022

Citation:

Berger TMI, Michaelis C, Probst I,
Sagmeister T, Petrowitsch L,
Puchner S, Pavkov-Keller T,
Gesslbauer B, Grohmann E and
Keller W (2022) Small Things Matter:
The 11.6-kDa TraB Protein is Crucial
for Antibiotic Resistance Transfer
Among Enterococci.
Front. Mol. Biosci. 9:867136.
doi: 10.3389/fmolb.2022.867136

¹Institute of Molecular Biosciences, Department of Structural Biology, University of Graz, Graz, Austria, ²Faculty of Life Sciences and Technology, Department of Microbiology, Berliner Hochschule für Technik, Berlin, Germany, ³Division of Infectious Diseases, University Medical Center Freiburg, Freiburg, Germany, ⁴Field of Excellence BioHealth, University of Graz, Graz, Austria, ⁵BioTechMed-Graz, Graz, Austria, ⁶Institute of Pharmaceutical Sciences, Division of Pharmaceutical Chemistry, University of Graz, Graz, Austria

Conjugative transfer is the most important means for spreading antibiotic resistance genes. It is used by Gram-positive and Gram-negative bacteria, and archaea as well. Conjugative transfer is mediated by molecular membrane-spanning nanomachines, so called Type 4 Secretion Systems (T4SS). The T4SS of the broad-host-range inc18-plasmid pIP501 is organized in a single operon encoding 15 putative transfer proteins. pIP501 was originally isolated from a clinical *Streptococcus agalactiae* strain but is mainly found in *Enterococci*. In this study, we demonstrate that the small transmembrane protein TraB is essential for pIP501 transfer. Complementation of a markerless pIP501 Δ traB knockout by traB lacking its secretion signal sequence did not fully restore conjugative transfer. Pull-downs with Strep-tagged TraB demonstrated interactions of TraB with the putative mating pair formation proteins, TraF, TraH, TraK, TraM, and with the lytic transglycosylase TraG. As TraB is the only putative mating pair formation complex protein containing a secretion signal sequence, we speculate on its role as T4SS recruitment factor. Moreover, structural features of TraB and TraB orthologs are presented, making an essential role of TraB-like proteins in antibiotic resistance transfer among Firmicutes likely.

Keywords: type IV secretion system, *Enterococcus*, plasmid, antibiotic resistance, conjugative transfer, secretion complex

INTRODUCTION

Currently, antibiotic resistances are one of the top global threats challenging the world. In recent decades, inappropriate prescription of antimicrobials in health-care settings and overuse along the food chain have led to an increased dissemination of antibiotic resistant (ABR) bacteria (Kim et al., 2021; Lin et al., 2021). Limitations in therapeutical treatment options harden the treatment success of patients with drug-resistant infections caused by hospital-acquired pathogens. The opportunistic Gram-positive (Gram+) pathogens *Enterococcus faecalis* and *Enterococcus faecium* cause the majority of healthcare-associated enterococcal infections (García-Solache and Rice, 2019;

Krawczyk et al., 2021; Levitus et al., 2022). Conjugative transfer, a type of horizontal gene transfer, is the major mechanism disseminating antibiotic resistance genes. It is mediated by mobile genetic elements, for example, integrative conjugative elements (ICEs) and conjugative plasmids encoding all the proteins required for their transfer themselves. Even though conjugative elements and their transfer processes are present in both Gram-negative (Gram-) and Gram+ bacteria, Gram-conjugation has been studied in more detail (Christie, 2016; Kohler et al., 2018b; Grohmann et al., 2018; Fischer et al., 2020). Profound knowledge on plasmid-mediated conjugation in Gram+ bacteria is highly needed (Alvarez-Martinez and Christie, 2009; Goessweiner-Mohr et al., 2014a; Kohler et al., 2018b; Grohmann et al., 2018; Costa et al., 2021). Membrane-spanning molecular nanomachines like Type IV secretion systems (T4SS) largely contribute to the dissemination of multi-resistant bacteria. They play a primary role in conjugative transfer in Gram- and Gram+ bacteria and are thereby involved in the pathogenesis of bacteria. The main function of T4SSs is the translocation of single-stranded plasmid DNA through the secretion channel, the so-called mating pair formation (MPF) complex, into the recipient.

The plasmid with the broadest known host range among Gram+ conjugative plasmids is the enterococcal plasmid pIP501 which was originally isolated from *Streptococcus agalactiae* (Horodniceanu et al., 1976). It belongs to the incompatibility (inc) group 18 (Palmer et al., 2010). Representatives of the inc18 family encode resistances to the macrolide, lincosamide, and streptogramin (MLS) group of antibiotics. The conjugation machinery of pIP501 is encoded by the ~15 kb-transfer (*tra*) operon consisting of 15 *tra* genes, *traA* to *traO*. The plasmid is capable of self-transfer and stable replication in virtually all Gram+ bacteria including *Enterococci*, *Staphylococci*, *Listeria* or *Streptomyces* and can transfer to Gram- *Escherichia coli* as well (Kurenbach et al., 2003; Kohler et al., 2018b). Seven putative VirB/D4 orthologs of the prototype *Agrobacterium tumefaciens* T4SS have been identified in pIP501 (Grohmann et al., 2003; Goessweiner-Mohr et al., 2014a; Grohmann et al., 2017) thereby representing one of the best-characterized T4SS in Gram+ bacteria (Li and Christie, 2018).

Expression of the 15 pIP501 *tra* genes is regulated by binding of the TraA relaxase to the main conjugation promoter P_{tra} (Grohmann et al., 2016). The pIP501 type IV coupling protein (T4CP) consists of two proteins, TraI and TraJ. TraI functions as membrane anchor while TraJ is the canonical coupling factor (Goessweiner-Mohr et al., 2014a). TraG is the VirB1-like lytic transglycosylase of the system. It locally cleaves the peptidoglycan and is involved in the assembly of the MPF proteins (Arends et al., 2013; Kohler et al., 2018b). Eight of the Tra proteins, TraB, TraC, TraF, TraH, TraI, TraK, TraL, and TraM, have been predicted to be involved in the formation of the MPF complex (Kohler et al., 2018b), for example, the two VirB8 orthologs, TraH and TraM, which were postulated to be part of the translocation channel (Kohler et al., 2017; Kohler et al., 2018b). The small cytosolic TraN protein was characterized as conjugation repressor and transcriptional regulator of the *tra* operon. *traN* deletion resulted in enhanced conjugative transfer (Kohler et al., 2018a).

In this study, we focused on the small transmembrane protein TraB. The processed *traB* gene product codes only for 80 amino acids, making it the smallest member of the Tra_{pIP501} protein family. We proved that TraB is essential for pIP501 transfer, present its structural features and discuss its putative role in the T4SS complex.

MATERIALS AND METHODS

Bacterial Strains and Growth Conditions

The bacterial strains and plasmids used in this study are listed in **Supplementary Table S1**. *Escherichia coli* and *Bacillus megaterium* strains as plasmid hosts were cultured in lysogeny broth (LB) under shaking at 37°C, for *B. megaterium* strains baffled flasks were used. *Enterococcus faecalis* strains were routinely grown in brain heart infusion (BHI) broth at 37°C with shaking. 1% w/v agar was added for preparing solid media. For selection, antibiotics were added as indicated in **Supplementary Table S1**.

Construction of a *traB* in-Frame Deletion Mutant in pIP501

A pIP501 $\Delta traB$ in-frame deletion mutant was constructed in *E. faecalis* JH2-2 using the previously described markerless allelic exchange strategy (Kristich et al., 2007). Oligonucleotides were purchased from Thermo Fisher and are listed in **Supplementary Table S2**. Restriction enzymes were purchased from New England Biolabs, as well as T4 DNA ligase and Phusion DNA polymerase. The first recombinant construct for *traB* in-frame deletion was generated by amplifying *traB* upstream and downstream flanking regions (1,007 bp and 1,054 bp, respectively) using *E. faecalis* JH2-2 (pIP501) as template with primers containing PstI/XbaI restriction sites for the upstream fragment and BamHI/EcoRI for the downstream fragment. The fragments were sequentially cloned into pUC18 using the corresponding restriction sites to create pUC18-UPS-DWS-*traB*. *E. coli* DH5 α was transformed with the recombinant DNA, clones were selected on LB agar with 100 μ g/ml ampicillin. More than 96% of the *traB* coding region was deleted retaining only two intact N-terminal and C-terminal codons of *traB* to prevent polar effects on downstream *tra* genes. The fused flanking regions were excised from pUC18 by digestion with PstI and EcoRI and inserted into the equally digested suicide plasmid pKA, followed by transformation into *E. coli* EC1000, resulting in pKA-UPS-DWS-*traB*. Clones were selected on BHI agar containing 250 μ g/ml erythromycin. The correctness of all plasmid constructs was confirmed by Sanger sequencing (Eurofins Genomics Germany GmbH, Ebersberg, Germany). Electrocompetent *E. faecalis* JH2-2 (pIP501) cells were transformed with pKA-UPS-DWS-*traB* by electroporation with a Bio-Rad GenePulser X-Cell using 0.2 cm gap width cuvettes and settings of 2,000 kV, 200 Ω , and 25 μ F. Transformants were selected on BHI agar supplemented with 50 μ g/ml fusidic acid, 20 μ g/ml chloramphenicol, 20 μ g/ml erythromycin, 100 μ g/ml gentamicin, coated with 100 μ l of a 20 mg/ml 5-bromo-4-chloro-3-indolyl- β -D-galactopyranoside

(X-gal) solution. Blue colonies were screened for homologous integration of pKA-UPS-DWS-*traB* into pIP501 by PCR. Colonies with integrated pKA-UPS-DWS-*traB* were grown in BHI medium supplemented with 50 µg/ml fusidic acid and 20 µg/ml chloramphenicol three times to stationary phase and finally until an OD₆₀₀ of 0.4. Serial dilutions were spread on MM9YEG agar plates supplemented with 50 µg/ml fusidic acid, 20 µg/ml chloramphenicol and 10 mM DL-p-chlorophenylalanine, coated with 100 µl 20 mg/ml X-gal solution. White colonies were screened for *traB* deletion by PCR. The pIP501Δ*traB* mutant was verified by sequencing of the deletion borders.

Complementation of *E. faecalis* JH2-2 (pIP501Δ*traB*)

For *traB* knockout complementation, the *traB* wild type gene with its ribosomal binding site (RBS) was amplified from pIP501 with primers containing BstYI/SalI restriction sites and inserted into the shuttle vector pEU327 followed by transformation into *E. coli* DH5α cells. Selection was carried out on LB agar with 100 µg/ml spectinomycin. For detection of C-terminally Strep-tag II-coupled TraB proteins and complementation studies a linker, a C-terminal Strep-tag II coding sequence (SA-WSHPQFEK) and a stop codon were inserted into pEU327 by using the site-directed mutagenesis kit (Q5 site-directed mutagenesis kit, New England Biolabs, Frankfurt am Main, Germany) according to the manufacturer's instructions using the primers pEU327_Mut_C-Strep fw and pEU327_Mut_C-Strep rev. After DpnI treatment the nicked DNA was transformed into *E. coli* DH5α cells, resulting in pEU327 containing the C-terminal Strep-tag (pEU327-Strep). To incorporate the *traB* gene with its native RBS into pEU327-Strep, a Gibson Assembly Kit (New England Biolabs) was applied. The primers used for amplification of pEU327-Strep (GA_pEU327_CStrep fw and GA_pEU327_CStrep rev) and *traB* including its RBS (GA_RBS-*traB* fw and GA_RBS-*traB* rev) as well as all other primers used for cloning or sequencing are listed in **Supplementary Table S2**. The protocol was carried out according to the manufacturer's instructions, resulting in pEU327-RBS-*traB* with a C-terminal Strep-tag (pEU327-RBS-*traB*-Strep). pEU327-RBS-*traB* was used to delete the *traB*₂₋₃₀ sequence by Q5 site-directed mutagenesis according to the manufacturer's instructions using the primers Mut_pEUtraB31-110 fw and Mut_pEUtraB31-110 rev, resulting in pEU327-RBS-*traB*₃₁₋₁₁₀. For biparental mating assays, *E. faecalis* JH2-2 (pIP501Δ*traB*) was electroporated with either pEU327-RBS-*traB*, pEU327-RBS-*traB*-Strep or pEU327-RBS-*traB*₃₁₋₁₁₀ as described in *Construction of a traB in-Frame Deletion Mutant in pIP501* Selection for *E. faecalis* JH2-2 (pIP501Δ*traB*; pEU327-RBS-*traB*), *E. faecalis* JH2-2 (pIP501Δ*traB*; pEU327-RBS-*traB*-Strep) and *E. faecalis* JH2-2 (pIP501Δ*traB*; pEU327-RBS-*traB*₃₁₋₁₁₀) was conducted on BHI agar with 20 µg/ml chloramphenicol, 20 µg/ml erythromycin and 500 µg/ml spectinomycin. Transformants were confirmed by PCR analysis.

Biparental Mating Assay

Biparental mating assays were performed with isogenic *E. faecalis* (pIP501), *E. faecalis* (pIP501Δ*traB*), *E. faecalis* (pIP501Δ*traB*; pEU327-RBS-*traB*), *E. faecalis* JH2-2 (pIP501Δ*traB*, pEU327-RBS-*traB*-Strep) and *E. faecalis* JH2-2 (pIP501Δ*traB*, pEU327-

RBS-*traB*₃₁₋₁₁₀) as donor strains and *E. faecalis* OG1X as plasmid-free recipient as described in Fercher et al. (2016). Transconjugants were selected on BHI agar supplemented with 1.5 mg/ml streptomycin and 20 µg/ml erythromycin. All mating assays were performed in quadruplicates. Transfer rates (number of transconjugants per recipient cell) are given with standard deviation. Significance and *p*-values were calculated with the Welch's *t* test. Significance is indicated by asterisks: ****p* < 0.0003, ***p* < 0.0038.

Cloning of *traB*

Based on the secondary structure prediction of TraB a truncation variant of *traB* was generated, lacking the secretion signal sequence. It was denominated TraB₃₁₋₁₁₀ referring to the amino acids present in the truncated protein. The 243-bp *traB*₃₁₋₁₁₀ PCR product was cut with BamHI and HindIII (New England Biolabs) and ligated into the expression plasmid pQTEV cut with the same enzymes. pQTEV contains a tobacco etch virus (TEV) protease-cleavable His-tag. The recombinant plasmid was transformed into *E. coli* BL21-CodonPlus (DE3)-RIL and BL21 star (DE3). The correctness of the *traB*₃₁₋₁₁₀ sequence was verified *via* Sanger sequencing by Microsynth AG (Balgach, Switzerland). All primers used for cloning and sequencing are listed in **Supplementary Table S2**.

TraB₃₁₋₁₁₀ Expression and Test Purification

TraB₃₁₋₁₁₀ was expressed in BL21 star (DE3) and *E. coli* BL21 CodonPlus (DE3)-RIL cells in LB medium supplemented with ampicillin (100 µg/ml) and in addition with chloramphenicol (32 µg/ml) for *E. coli* BL21 CodonPlus (DE3)-RIL under shaking with 180 rpm. At an OD₆₂₀ of ~0.7 TraB₃₁₋₁₁₀ expression was induced by adding 0.5 mM IPTG. Incubation continued for 16 h at 30°C under shaking. Cells expressing TraB₃₁₋₁₁₀ were harvested by centrifugation at 9,000 × *g* for 40 min. The pellet was resuspended in lysis buffer (50 mM Tris/HCl, 150 mM NaCl, 20 mM imidazole, 2% Tween-20, pH 8.0, filtered using a MF-Millipore™ 0.45 µm MCE membrane (Merck, Darmstadt, Germany) containing protease inhibitor (Pierce protease Inhibitor Tablets, Thermo Fisher Scientific, Waltham Massachusetts, United States). After homogenization the cells were disrupted by sonication (50% duty cycle, 60% intensity, Sonopuls HD 2070 ultrasonic probe) on ice four times for 16 min each with 8 min breaks in between. The disrupted cells were centrifuged in a Beckman Coulter Avanti J-26 XP centrifuge (Brea, California, United States) using a JA 25.50 rotor at 38,000 × *g* for 40 min. The supernatant was filtered through a PVDF Rotilabo® syringe filter with a pore size of 0.45 µm (Carl Roth GmbH + Co. KG, Karlsruhe, Germany) and loaded onto a 5-ml HisTrap™ HP column (Cytiva, Marlborough, Massachusetts, United States) and purified by an ÄKTA FPLC system. Test purification was monitored on a 12% SDS polyacrylamide gel using Lämmli standard buffer conditions (Laemmli, 1970).

TraB₃₁₋₁₁₀ Purification

All purification steps were performed on an ÄKTA FPLC system. Elution fractions of the nickel-based immobilized metal affinity chromatography (Ni-IMAC) were pooled and applied to dialysis using a dialysis tube (Spectra/Por® 3, Repligen, Waltham, Massachusetts, United States) with a molecular weight (MW)

cutoff of 3.5 kDa. TraB₃₁₋₁₁₀ was cleaved by TEV protease and dialyzed against 50 mM Tris/HCl, 150 mM NaCl and 2 mM DTT for 2 days. Cleaved TraB₃₁₋₁₁₀ was separated from uncleaved TraB₃₁₋₁₁₀ and TEV protease by performing a reverse Ni-IMAC using a 5-ml HisTrap™ HP column at a flow rate of 3 ml/min. As last purification step, a size exclusion chromatography (SEC) using a Superdex 200 increase 10/300 (Cytiva) column at a flow rate of 0.3 ml/min was performed.

Construction of Plasmids for Expression of pIP501 *tra* Operon Proteins in *B. megaterium*

Polycistronic expression of *traB-traO*_{pIP501} in *B. megaterium* MS941 was carried out with the *B. megaterium/E. coli* shuttle vector pMGBm19 containing *traB* to *traO*. *traB* with a C-terminal Strep-tag II and a ribosomal binding site was inserted into the *B. megaterium/E. coli* shuttle vector pRBBm59 to allow purification of TraB and its interaction partners *via* affinity chromatography.

traB to *traO*_{pIP501} was amplified using Q5 polymerase and primers pMGBm19-*traBO*_fw and pMGBm19-*traBO*_rev. The BamHI/SacI-digested insert was ligated into pMGBm19 cut with the same enzymes and transformed into One Shot™ TOP10 Chemically Competent *E. coli* cells, resulting in pMGBm19-RBS-*traB-traO*. Gibson Assembly (Gibson Assembly Kit, New England Biolabs) was used to insert RBS-*traB*-Strep into pRBBm59. pEU327-RBS-*traB*-Strep served as template for amplification of the insert. Prior to Gibson Assembly, *traB*-Strep was amplified with an added stop codon, an artificial RBS (AAAGGGGGAAA) and a BamHI restriction site as spacer on the 5' end using primers *traB*-pRBBm59 fw and *traB*-pRBBm59 rev, resulting in a 389 bp fragment. The amplicon was used as a template to produce the Gibson Assembly insert using the primers GA_*traB* CStrep prBB fw and GA_*traB* CStrep prBB rev. The backbone of pRBBm59 was amplified by using GA_pRBBm59 fw and GA_pRBBm59 rev primers and Q5 polymerase, generating a 5,750 bp fragment. The resulting construct was denominated pRBBm59-RBS-*traB*-Strep. The correctness of all plasmids generated was confirmed by Sanger sequencing. All primers used for cloning and sequencing are listed in **Supplementary Table S2**.

B. megaterium MS941 was co-transformed with pMGBm19-RBS-*traB-traO*, containing a xylose-inducible promoter and pRBBm59-RBS-*traB*-Strep, containing a sucrose-inducible promoter using a protoplast transformation protocol for *B. megaterium* (Biedendieck et al., 2011). Colonies were selected on LB agar containing 35 µg/ml chloramphenicol and 10 µg/ml tetracycline and were screened for the presence of the plasmids by colony PCR.

Expression and Purification of Strep-Tagged TraB and its Interaction Partners from *B. megaterium* MS941 (pMGBm19-RBS-*traB-traO*; pRBBm59-RBS-*traB*-Strep) Lysate

Overnight cultures of *B. megaterium* MS941 (pMGBm19-RBS-*traB-traO*; pRBBm59-RBS-*traB*-Strep) were grown in baffled

flasks in LB medium supplemented with chloramphenicol (35 µg/ml) and tetracycline (10 µg/ml) at 37°C and 250 rpm. Expression cultures (1 l in 5 l baffled flasks) were inoculated to an OD₆₀₀ of 0.05 in the same medium and incubated until an OD₆₀₀ of 0.3–0.4 at 37°C. Expression of TraB-TraO and Strep-tagged TraB was induced with 0.5% (w/v) xylose and sucrose, respectively, followed by incubation for 4 h. Cells were harvested at 9,000 × g at 4°C, lysed in 70 ml TraB-TraO/TraB-Strep binding buffer (50 mM Hepes, 300 mM NaCl, 1 mM EDTA, pH 7.5, 0.5% Nonidet® P 40 Substitute (NP-40) Proteomics Grade (AMRESCO, VWR Life Science) filtered through a MF-Millipore 0.45 µm MCE membrane (Merck, Darmstadt, Germany) supplemented with additional NP-40 up to 2% and protease inhibitor (Pierce protease Inhibitor Tablets, Thermo Fisher Scientific, Waltham Massachusetts, United States) using the SONOPULS HD 2070 ultrasonic homogenizer (BANDELIN electronic GmbH & Co. KG, Berlin, Germany) on ice for 60 min at 60% intensity and 50% duty cycle. After 60 min centrifugation at 4°C and 38,000 × g, the supernatant was passed through a 0.45 µm PVDF syringe filter (Merck Chemicals and Life Science GmbH, Vienna, Austria) prior to loading onto a 5-ml StrepTrap™ HP column pre-equilibrated with TraB-TraO/TraB-Strep binding buffer at 4°C using an ÄKTA pure 25 L chromatography system. The protein was eluted in a 60% gradient of TraB-TraO/TraB-Strep elution buffer (50 mM Hepes, 300 mM NaCl, 1 mM EDTA, 2.5 mM desthiobiotin). 2 ml fractions were collected. Peak fractions were loaded onto a 12% SDS polyacrylamide gel and subjected to immunoblotting using polyclonal anti-Tra antibodies directed against TraF, TraG, TraH, TraK, and TraM (Biogenes, Berlin, Germany) at a 1:10,000 dilution to probe for coeluted Tra proteins. As secondary antibody a horseradish peroxidase conjugated antibody against rabbit IgG (Promega GmbH, Mannheim, Germany) was used at a dilution of 1:10,000.

CD Measurements

CD measurements were performed on a J-1500 Circular Dichroism Spectrophotometer (JASCO Corporation, Tokyo, Japan). Far-UV CD spectra were recorded at 20°C from 260 to 180 nm with a data pitch of 0.2 nm and a bandwidth of 2 nm applying a scanning speed of 100 nm/min. Each spectrum was recorded as an average of 20 scans. The resulting spectra were baseline-corrected by subtracting the signal of the buffer. TraB₃₁₋₁₁₀ was prepared with a concentration of 0.15 mg/ml in 50 mM Tris/HCl, 150 mM NaCl, pH 8.0, 0.05% DDM. The CD signal was converted to mean residue ellipticity [θ] and secondary structure was determined with dichroweb using the CDSSTR algorithm (Compton and Johnson, 1986; Miles et al., 2022).

In Vitro Cross-Linking of TraB₃₁₋₁₁₀

50 µl samples of 10 µg TraB₃₁₋₁₁₀ in SEC buffer containing 0/0.001/0.01/0.05/0.1% glutaraldehyde in 50 mM Bicine, 150 mM NaCl, 1 mM DTT were incubated for 20 min at room temperature. Cross-linking was stopped by adding glycine to a final concentration of 140 mM followed by 5 min incubation at room temperature. 400 µl of –20°C-cold acetone was added and the samples were precipitated at –20°C for 2 h, followed by

centrifugation at $16,100 \times g$ for 15 min. Pellets were resuspended in 10 μ l distilled water and 10 μ l SDS-PAGE loading buffer. 15 μ l samples were loaded onto a 12% SDS polyacrylamide gel. Unstained protein MW marker (Thermo Fisher Scientific) was used to assess the size of the cross-linked oligomers.

Mass Spectrometry of Putative TraB₃₁₋₁₁₀ Bands

Putative TraB₃₁₋₁₁₀ bands were excised from a silver-stained 12% SDS polyacrylamide gel and subjected to in-gel reduction, alkylation and trypsinization as described previously (Gesslbauer et al., 2018). Extracted peptides were purified and concentrated using C18 spin columns (Pierce™ C18 Spin Columns; Thermo Fisher Scientific) according to the manufacturer's protocol.

The concentrated purified peptides were applied to Liquid Chromatography (LC) through an Ultimate 3,000 RSLCnano System (Thermo Fisher Scientific). Peptides were separated with a flow rate of 300 nl/min on a C18 Aurora UHPLC column (25 cm \times 75 μ m ID, 1.6 μ m) with CaptiveSpray Insert (IonOptics). The mobile phases were (A) 0.1% (v/v) formic acid in water and (B) 0.1% (v/v) formic acid in acetonitrile. The HPLC gradient for separation was 2% B for 6 min, 2–25% B for 90 min, 25–40% B for 10 min, 40–80% B for 10 min, 80% B for 10 min and 2% B for 12 min. The LC system was coupled online to a timsTOF Pro mass spectrometer (Bruker Corporation, Billerica, Massachusetts, United States) with CaptiveSpray nano-electrospray ion source (Bruker). The mass spectrometer was operated in PASEF mode. TIMS, PASEF and calibration settings were applied as described by Meier et al. (2018).

Mass spectrometry raw files were processed with MaxQuant version 1.6.15.0. MS/MS spectra were searched against the UniProt *E. coli* (K12) reference proteome databank (Proteome ID: UP000000625) (Cox and Mann, 2008). The TraB₃₁₋₁₁₀ sequence was manually included in the *E. coli* FASTA file. Search parameters were set as follows: trypsin was set as enzyme; a maximum of two missed cleavages was allowed; the minimum peptide sequence length was seven amino acids, and the maximum peptide mass was 4,600 Da. Carbamidomethylation of cysteine was set as a fixed modification; oxidation of methionine and acetylation of protein amino-termini were set as a variable modification. All other MaxQuant search parameters were equivalent to those described by Meier et al. (2018).

Structural Characterization of TraB

The following online services were used to search for transmembrane motifs in the TraB sequence and potential orthologous proteins: PSIPRED 4.0 (Buchan and Jones, 2019; Moffat and Jones, 2021), MEMPACK (Nugent et al., 2011), DomPred (Bryson et al., 2007), MEMSAT-SVM (Nugent and Jones, 2009). PSIPRED was used to predict the secondary structure content of TraB and orthologous proteins. After identifying seven TraB orthologs by an iterative PSI-BLAST using the NCBI database, a multiple sequence alignment with T-Coffee was performed using the PSI/TM-Coffee function for

membrane proteins (Notredame et al., 2000; Chang et al., 2012). The multiple sequence alignment and the structural categorization were evaluated with the implemented TCS tool (Chang et al., 2014; Chang et al., 2015). General features of the recombinant TraB₃₁₋₁₁₀ constructs were assessed with ProtParam (Gasteiger et al., 2005). RoseTTAFold was used for 3D structure prediction of TraB and its putative orthologs (Baek et al., 2021). PyMOL Molecular Graphics System, Version 2.5 was used for the presentation of the theoretical structures and their alignment using the method “cealign” (Shindyalov and Bourne, 1998).

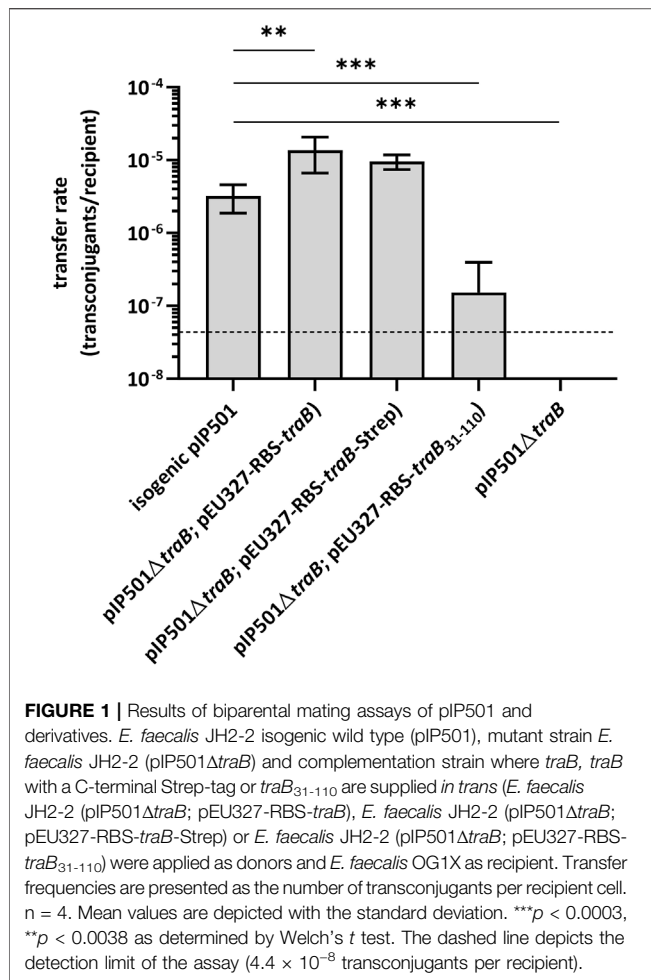
Subcellular Localization of TraB in *E. faecalis*

Subcellular fractionation of *E. faecalis* JH2-2 (pIP501), *E. faecalis* JH2-2 (pIP501 Δ traB), and *E. faecalis* JH2-2 (pIP501 Δ traB, pEU327-RBS-*traB*-Strep) was performed as described in Goessweiner-Mohr et al. (2013) with some modifications. Cultures were diluted to an OD₆₀₀ of 0.05 in BHI medium containing 20 μ g/ml chloramphenicol, for the pEU327 derivative, additionally supplemented by 500 μ g/ml spectinomycin and incubated at 37°C until an OD₆₀₀ of 0.5 was reached. The culture was kept on ice for 15 min and centrifuged for 10 min at 4°C at $6,000 \times g$. The pellet was washed twice with 10 ml 50 mM KH₂PO₄/K₂HPO₄ buffer (50 mM, pH 7) and resuspended in 1 ml lysis buffer (50 mM KH₂PO₄/K₂HPO₄, pH 7, 1 mM EDTA, 1 mM MgCl₂, 100 μ g/ml RNase, 1 U/ μ l DNase, 1:1000 diluted protease inhibitor [stock solution: 1 mg/ml pepstatin, 2 mg/ml antipain, 20 mg/ml leupeptin], 1 mg/ml lysozyme). Unlysed material was removed by centrifugation at $1,000 \times g$ for 2 min at 4°C. The supernatant was centrifuged at $16,000 \times g$ for 20 min at 4°C. The resulting pellet corresponding to the cell wall fraction was resuspended in 100 μ l potassium phosphate buffer (50 mM KH₂PO₄/K₂HPO₄, pH 7). The supernatant was applied to ultracentrifugation at $163,000 \times g$ for 2 h at 4°C. The resulting pellet representing the membrane fraction was resuspended in 100 μ l potassium phosphate buffer (50 mM KH₂PO₄/K₂HPO₄, pH 7) containing 1% Triton X-100. The supernatant containing the cytoplasmic fraction was reduced to a final volume of 100 μ l by vacuum centrifugation in a centrivap concentrator (LABCONCO, Kansas City, Missouri, United States). TraB was probed in the cell wall, cell membrane, and cytoplasmic fraction by western blotting using a polyclonal antibody directed against TraB₃₁₋₁₁₀ (Proteogenix SAS, Schiltigheim, France) in a dilution of 1:8,000. The same protocol was used as described in (*Expression and Purification of Strep-Tagged TraB and its Interaction Partners from B. megaterium MS941 (pMGBm19-RBS- traB-traO; pRBBm59-RBS-traB-Strep) Lysate*), with the difference that no detergent was used processing the membrane.

RESULTS

TraB is Essential for pIP501 Transfer

To study the role of the transmembrane protein TraB in pIP501 conjugative transfer, biparental mating assays were conducted with the *E. faecalis* JH2-2 (pIP501 Δ traB) deletion mutant as donor and *E. faecalis* OG1X as recipient. The transfer



frequency of the deletion mutant was below the detection limit of the assay ($<4.4 \times 10^{-8}$ transconjugants per recipient). As *traB* deletion resulted in a total loss of plasmid transfer, TraB proved to be essential for pIP501-mediated conjugative transfer (Figure 1).

Complementation of the *traB* knockout by supplying the wild type *traB* gene *in trans* showed full recovery of transfer with transfer frequencies close to wild type level thus excluding polar effects of the deletion on downstream *tra* genes. Similar transfer rates were observed, when supplying the wild type *traB* gene with a C-terminal Strep-tag (*traB*-Strep) *in trans*. Thus, the Strep-tag did not impact the functionality of TraB. Complementation of the deletion mutant by supplying a truncated *traB*₃₁₋₁₁₀ variant lacking the N-terminal secretion signal sequence *in trans* resulted in a significantly diminished transfer rate in comparison to the wild type pointing to a crucial role of the signal sequence as correct localization of TraB is substantial in the transfer process.

TraB is an α -Helical Transmembrane Protein

Combining the secondary structure prediction of PSIPRED and the analysis with MEMPACK, MEMSAT-SVM and SignalP5.0 a scheme of the TraB domain composition was built (Nugent and

Jones, 2009; Nugent et al., 2011; Almagro Armenteros et al., 2019; Buchan and Jones, 2019; Moffat and Jones, 2021) (Figure 2). Although TraB is predicted to contain three α -helices, the mature TraB₃₁₋₁₁₀ only contains two membrane spanning helices as the first helix spanning from lysine 2 to phenylalanine 23 belongs to a secretion signal sequence, which is cleaved off between alanine 30 and alanine 31.

The first transmembrane helix (TMH1) starts at proline 34 and stops at proline 70. It is predicted to enter the membrane at asparagine 43 and leaves the membrane at isoleucine 64. Lysine 67 might interact with the phospholipid headgroup and tyrosine 68 as a membrane anchor. The loop connecting TMH1 and TMH2 is facing into the cytosol. TMH2 starts with proline 75, is predicted to enter the cell membrane at leucine 85 and to leave it at tyrosine 106. Tryptophane 104 probably serves as membrane anchor. The possible function of some particular amino acids will be discussed in more detail in the following chapters.

TraB_{pIP501} Localizes in the Cell Envelope

Subcellular localization by cell fractionation revealed that TraB_{pIP501} is found in the cell wall fraction and in the cell membrane fraction. This has been shown for *E. faecalis* JH2-2 (pIP501) as well as for the complementation strain *E. faecalis* JH2-2 (pIP501ΔtraB, pEU327-RBS-*traB*-Strep). The *traB* deletion strain *E. faecalis* JH2-2 (pIP501ΔtraB) served as negative control. The Western Blot is shown in Figure 2, panel C.

TraB Orthologs Were Found on Type IV Secretion Systems from Diverse Firmicutes

We used the NCBI database to search for TraB_{pIP501} orthologs. The results are shown in Table 1. Interestingly, TraB orthologs were detected on numerous bacterial strains belonging to the phylum Firmicutes, including nosocomial pathogens such as MRSA, *S. aureus*, *E. faecalis* as well as biotechnologically relevant bacteria such as *Lactococcus lactis* and environmental species like *Clostridium algarophilum*. Their identities range from 42 to 100% identity on amino acid level. All *traB* orthologs were found in gene clusters encoding a putative T4SS, several of them on conjugative plasmids, namely on the broad-host-range inc18 plasmids, pRE25 and pAM β 1 (TraB orthologs with 100% identity on amino acid level; the other Tra orthologs show identities in the range of 74–100%) from *E. faecalis*, on the pSK41/pGO1-family plasmid pV030-8 from *S. aureus* and on the pNP40-like plasmid pUC11B from *Lactococcus lactis* (Ortiz Charneco et al., 2021). All of them are small proteins containing 101 to 114 amino acids in their unprocessed form. Their mature form is even more similar regarding their size ranging from 80 to 83 amino acids.

Figure 2, panel B shows a multiple sequence alignment generated by PSI/TM-Coffee of TraB_{pIP501} and its orthologs presented in Table 1. The accession numbers of the respective proteins are given. Table 1 gives both, the accession number, and the name of the respective gene product. The multiple sequence alignment suggests which parts of the proteins are inserted into the membrane. All TraB orthologs show the same pattern according to their insertion into the membrane, with the N- and C-terminal region pointing to the extracellular space and a

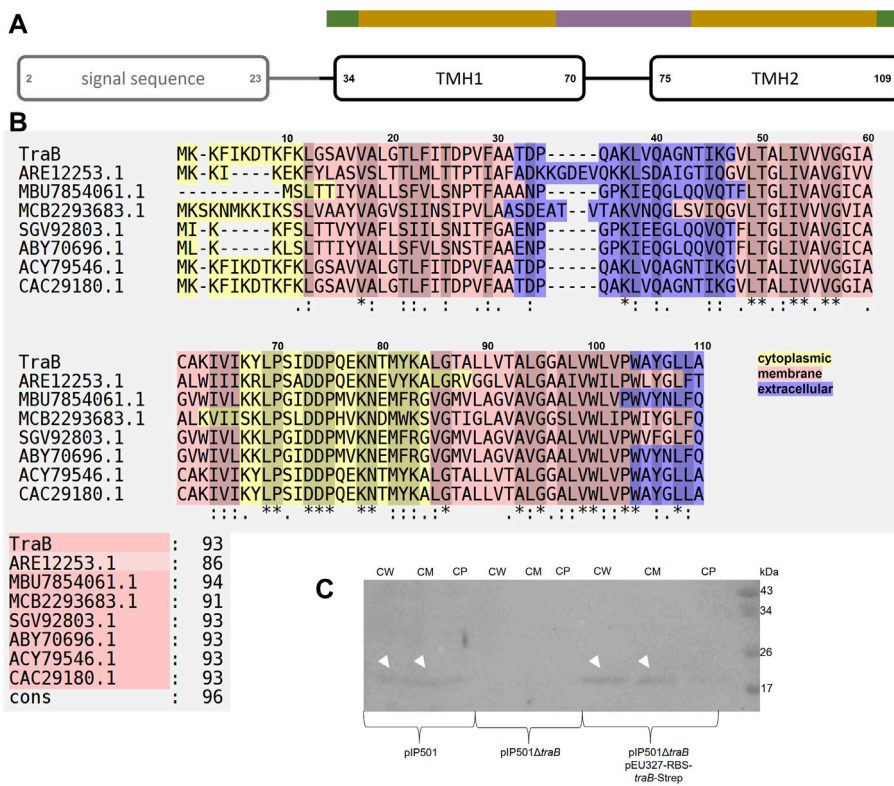


FIGURE 2 | (A) Domain composition of TraB. The first predicted helix is part of the secretion signal sequence (predicted with SignalP5.0) including a cleavage site between alanine 30 and alanine 31. Secondary structure elements were calculated with PSIPRED. After a short coil structure, the first transmembrane helix (TMH1) spans from proline 34 to proline 70 followed by a short loop region leading to the second transmembrane helix (TMH2) starting at proline 75 and ending at leucine 109. MEMPACK and MEMSAT-SVM were used to determine the orientation of TraB in the membrane as represented by the color code above the TMHs. Green parts are predicted to be extracellular, golden parts within the membrane and the lavender part intracellular. **(B)** Multiple sequence alignments using PSI/TM-Coffee for membrane proteins from the T-coffee server of TraB and its orthologs from other putative conjugative systems. Orthologs were identified by an iterative PSI-BLAST using the NCBI databank. Only proteins originating from a conjugative context were included in the multiple sequence alignments. The color scheme shows the orientation of the proteins mapped on to their sequence. The panel to the right shows the evaluation scores from the TCS evaluation. Asterisks "*" show conserved amino acids in all sequences. Colons ":" indicate amino acids of high similarities. Dots "." indicate partial similarities. In addition, identical and highly similar amino acids are highlighted with grey shading of the respective alignment boxes. The numbers above the aligned sequences are referring to the amino acid position of TraB_{pIP501}. **(C)** Western Blot of the cell fractionation of *E. faecalis* JH2-2 harboring different plasmids using a specific antibody against TraB_{pIP501}. The plasmids are given below the membrane. The fractions are labeled as: CW: cell wall; CM: cell membrane; CP: cytoplasm. TraB (white arrow heads) shows an unusual migration behavior with an apparent MW of 20 kDa on the SDS-PAGE, which is commonly observed for membrane proteins and may be explained by the atypical SDS binding (Rath et al., 2009).

TABLE 1 | TraB_{pIP501} and its orthologs found with PSI-BLAST using the NCBI database.

origin	Accession Number	Length (aa)	Query Coverage [%]	identity [%]	Gene Product
pIP501	AAA99467.1	110	—	—	TraB _{pIP501}
pUC11B	ARE12253.1	111	70	57.14	mating channel formation protein
<i>Staphylococcus aureus</i> AF2236	MBU7854061.1	101	90	45.45	CagC family T4SS protein
<i>Clostridium algariphilum</i> DSM 16153	MCB2293683.1	114	90	45.0	CagC family T4SS protein
<i>Staphylococcus aureus</i> 3688STDY6124879	SGV92803.1	105	93	41.75	TraB
pV030-8	ABY70696.1	105	92	44.12	TrsB
pAMβ1	ACY79546.1	110	100	100	TrsB
pRE25	CAC29180.1	110	100	100	TrsB

If encountered on a plasmid, the plasmid name is given, if location of the gene (genome or plasmid) is not specified, the bacterial strain is given. The table includes the length of the orthologs in number of amino acids (aa), the name/putative function of the protein. All orthologs are part of a putative type IV secretion system gene cluster.

loop region connecting two transmembrane helices facing into the cytoplasm (note: The amino acids 2–23 of TraB comprise the signal sequence). The evaluation with the in the T-Coffee package implemented calculation of the transitive consistency score (TCS) shows a high score for every protein sequence, rendering the prediction and the multiple sequence alignment reliable (Chang et al., 2014; Chang et al., 2015). The mating channel formation protein from pUC11B shows the lowest overall identity with TraB_{pIP501}, which is also reflected by the TCS evaluation. The largest sequence differences are located at the N-terminal part containing the secretion signal sequences. The best-conserved region is the part facing into the cytoplasm, although it has a difference of two amino acids in length. The second transmembrane helix of TraB from *Staphylococcus aureus* 3688STDY6124879 and the CagC family T4SS protein of *Clostridium algariphilum* DSM 16153 seem to be longer than the second transmembrane helix of the other ones.

The Theoretical Structures of TraB and Its Orthologs Show High Similarity

To obtain a more detailed picture of the 3D structure of the membrane-inserted TraB protein and its orthologs we generated structural models using the Robetta server (<https://robetta.bakerlab.org>). The recently available deep learning-based modeling method RoseTTAFold enables the ab-initio generation of structural models, which are quite accurate and do not require known homologous structures (Baek et al., 2021). The structures of TraB and the seven orthologs showed a very similar overall structure with the 2 TM helices arranged in an antiparallel manner and connected by a short and structurally defined loop. The signal helix, which is connected to TMH-1 via a longer, flexible loop exhibited the largest deviations in the alignment shown in **Figure 3**, panel A. The pairwise alignment to TraB_{pIP501} was performed with the alignment function using the cealign algorithm of *PyMOL 2.5* and yielded r.m.s.-deviations between 2.17 Å for the MPF protein from pUC11B over 80 atoms and 4.62 Å for TraB from *Staphylococcus aureus* 3688STDY6124879 over 104 atoms (Schrödinger and DeLano, 2020), *PyMOL* was retrieved from <http://www.pymol.org/pymol>. After removal of the secretion signal sequence the mature TraB protein consists of the two antiparallel TM helices, with a short flexible stretch at the N-terminal side of TMH-1 and the C-terminal end of TMH-2. The length of the two helices differs slightly (55 Å for TMH-1 and 50 Å for TMH-2) and matches quite well the secondary structure prediction and the expected length of a membrane spanning helix (Phillips, 2018). TMH-1 is straight, whereas TMH-2 features a pronounced kink in its C-terminal part, which is due to a conserved proline residue (P103 in TraB_{pIP501}). The two TMHs are connected by a tight loop (P70 to P75), which constitutes one of the highest conserved regions in the multiple sequence alignment (**Figure 3B**, panel B).

The TM helices exhibit a distinct distribution of hydrophilic and hydrophobic residues: in the middle part (colored in salmon in **Figure 3**, panel B, C and D) there are mainly hydrophobic

amino acids and no charged ones; the outer and inner parts (slate and yellow in **Figure 3**, panel B, C and D) consist of mainly hydrophilic residues, a large portion of which is charged. Both the outer and the inner parts carry a net positive charge, which is more pronounced for the inner part—including the TMH connecting loop, there are 5 lysines and 3 acidic residues (2 aspartates and 1 glutamate) in this region. The lysines are oriented closer to the central part of the TMHs consistent with their proposed membrane anchoring function (Landolt-Marticorena et al., 1993; Planque et al., 1999). The C-terminal part of TMH-2 has distinct features as it contains no charged amino acids but 3 aromatic residues, 2 tryptophanes and 1 tyrosine, which are clustered around the kink caused by P103. The two tryptophanes (W100 and W104 in TraB_{pIP501}) are conserved among all compared TraB-like proteins and most likely play an important role in membrane anchoring (Landolt-Marticorena et al., 1993; Planque et al., 1999) and/or protein-protein interaction within the MPF complex. The completely conserved residues including the two tryptophanes are shown in **Figure 3**, panel B. For better visualization, we zoomed into the regions containing the conserved residues and labeled them referring to their position within TraB_{pIP501}. This is shown in **Figure 3**, panel C for the outwards facing parts of TraB_{pIP501} and in panel D for the cytosolic loop region.

In Vitro Cross-Linking Revealed TraB Oligomers in the Range of Dimers to Tetramers

TraB₃₁₋₁₁₀ encoded on pQTEV-*traB*₃₁₋₁₁₀ was expressed in two different *E. coli* expression strains, BL21-CodonPlus (DE3)-RIL and BL21 star (DE3). A test purification, where the protein was isolated by a Ni-IMAC was performed to evaluate expression levels. As the isolated protein migrated slower than expected for its calculated MW, we performed MS analysis confirming that the band at 16 kDa corresponds to TraB₃₁₋₁₁₀. The examined bands are shown in **Figure 4**, panel A. As the TraB₃₁₋₁₁₀ band was more prominent using BL21-CodonPlus (DE3)-RIL cells for expression, they were used for large-scale expressions and purification. **Figure 4**, panel B shows the different purification steps of TraB₃₁₋₁₁₀. Lanes 1 and 2 show the pooled elution fractions from the Ni-IMAC step before and after dialysis and TEV cleavage, respectively. TEV cleavage was performed for 2 days, because detergents might compromise the cleavage efficiency of the TEV protease. This appeared to be the case for the used Tween-20 as only about 50% of TraB₃₁₋₁₁₀ was cleaved even after 2 days. Next, a reverse Ni-IMAC was performed to separate TEV-cleaved TraB₃₁₋₁₁₀ from uncleaved TraB₃₁₋₁₁₀ as well as from the TEV protease. Lanes 3 and 4 show the elution fractions of the reverse Ni-IMAC, containing impurities binding nonspecifically to the column, uncleaved TraB₃₁₋₁₁₀ and TEV-protease. The flow through was collected, concentrated, and loaded on to a Superdex 200 increase column to obtain TraB₃₁₋₁₁₀ of higher purity (lanes 6–10 of **Figure 4**, panel B). Lane 6 represents the peak eluting in the void volume of the column, containing highly aggregated impurities. TraB₃₁₋₁₁₀ eluted as a single peak at an elution volume of 12.3 ml (lanes 7–10) corresponding to a calculated MW of 172 kDa. This represents

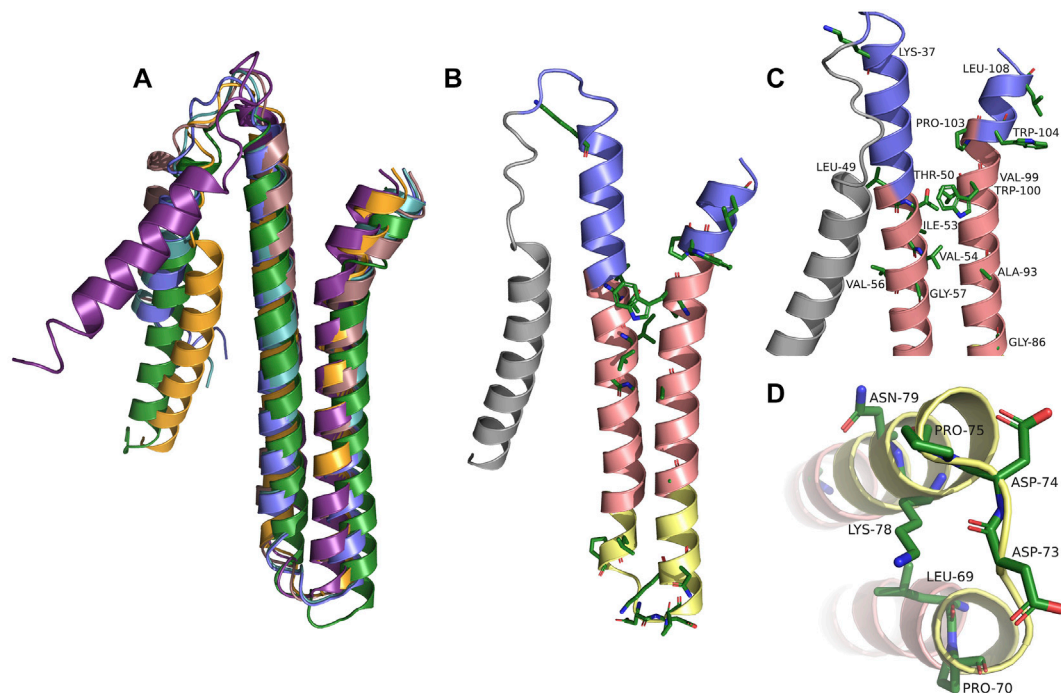


FIGURE 3 | (A) Alignment of TraB_{pIP501} and its orthologs using the theoretical structures from Robetta. TrsB_{pAM81} and TrsB_{pRE25} were not included, because both are 100% identical to TraB_{pIP501}. TraB_{pIP501} is shown in orange; the mating channel formation protein from pUCB11B is shown in purple; the CagC family protein from *Staphylococcus aureus* AF2236 is shown in rose; the CagC family protein from *Clostridium algariphilum* DSM 16153 is depicted in green; TraB from *Staphylococcus aureus* 3688STDY6124879 is shown in slate; TrsB_{pV030-8} is depicted in green-blue. **(B)** Shows TraB_{pIP501} colored according to its orientation in the cell membrane. The grey part represents the secretion signal sequence; slate parts the extracellular part; the salmon parts are predicted to be within the membrane; the yellow parts are cytosolic. Amino acids, which are conserved in the multiple sequence alignments are shown in stick presentation. **(C)** and **(D)** Zoom into the areas of TraB_{pIP501} showing the highest conservation. The conserved amino acids are shown as sticks and labeled. Same color scheme as in panel **(B,C)** Showing the details of the interface area between the cell membrane and the peptidoglycan layer. **(D)** Zoom into the cytosolic loop of TraB_{pIP501}, bottom view.

the micelle bound TraB₃₁₋₁₁₀. For further analysis like *in vitro* cross-linking or CD measurements only the main fractions containing TraB₃₁₋₁₁₀ in the highest purity were used. The CD spectrum in **Figure 4**, panel C indicates mainly α -helical content and no β -strand which agrees with the structural features obtained from the secondary structure predictions of TraB₃₁₋₁₁₀ (see *TraB is an α -Helical Transmembrane Protein*).

The results of the *in vitro* cross-linking are shown in **Figure 5**. At a glutaraldehyde concentration of 0.01% a dimer and trimer band become clearly visible, and a faint band of a tetramer appears. At a crosslinker concentration of 0.05% the distribution is shifted towards the trimer and tetramer. At the highest glutaraldehyde concentration (0.1%) unspecific cross-linking occurred leading to an indistinguishable variety of aggregates of different sizes. These results indicate that TraB₃₁₋₁₁₀ forms oligomers in Tween-20 micelles in a range from dimers to tetramers.

TraB is Likely Part of the pIP501 MPF Complex

As a predicted membrane protein, TraB is a likely candidate to interact with other T4SS proteins to assemble the translocation channel. A pull-down approach was used to elucidate the TraB interaction partners. The co-transformed *B. megaterium* MS941

strain expressed both, C-terminally Strep-tagged TraB (TraB-Strep) and the *tra*_{pIP501} operon proteins TraB to TraO. The C-terminal Strep-tag does not impact the functionality of TraB, as demonstrated by wild type transfer frequencies for the pIP501 *traB* knockout strain complemented with TraB containing a C-terminal Strep-tag (*E. faecalis* JH2-2 (pIP501 Δ *traB*, pEU327-RBS-*traB*-Strep) (**Figure 1**). TraB-Strep and interacting proteins were purified from the clarified supernatant of *B. megaterium* MS941 (pMGBM19-RBS-*traB*-*traO*; pRBBm59-RBS-*traB*-Strep) lysate *via* affinity chromatography. The putative MPF proteins TraF, TraH, TraM and TraK coeluted with TraB-Strep and were detected by immunoblotting (**Figure 6**). The cytosolic protein TraN and the putative surface adhesion protein TraO were used as negative controls. None of them was coeluted, as depicted for TraO (**Figure 6**). The two bands visible on the membrane incubated with anti-TraK antibody are due to two different translational start codons for TraK, resulting in the expression of two TraK variants differing by 4.1 kDa in size (Goessweiner-Mohr et al., 2014b). The two bands representing TraO are probably showing two differently processed forms. Unprocessed TraO has a MW of 29.9 kDa containing a putative secretion signal sequence with a cleavage site between alanine 24 and aspartic acid 25. Secreted TraO shows a MW of 27.4 kDa. The membrane incubated with

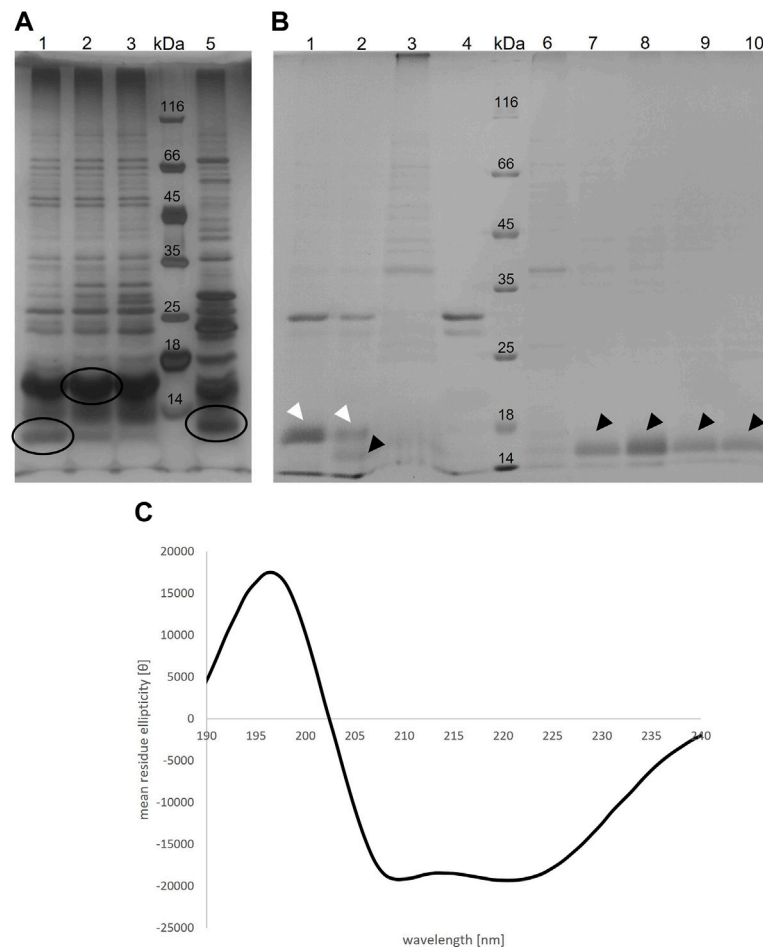


FIGURE 4 | (A) Silver-stained 12% SDS polyacrylamide gel of the elution fractions from IMAC of the TraB₃₁₋₁₁₀ test purification with two different *E. coli* expression strains. For lane 1-3 BL21 Codon Plus RIL cells were used, for lane 5 BL21 star cells. Lane 4 shows the MW standard (Thermo Fisher Scientific). Circled bands were cut out and applied to MS analysis **(B)** Coomassie-stained 12% SDS polyacrylamide gel showing different purification steps of TraB₃₁₋₁₁₀. Lane 1: pooled elution fraction of the IMAC; lane 2: same fractions after TEV cleavage; lane 3 and 4: elution fractions of the reverse IMAC; lane 5: MW standard (Thermo Fisher Scientific); lane 6-10: elution fractions of the SEC using a Superdex 200 increase column. White arrow heads point at uncleaved TraB₃₁₋₁₁₀. Black arrow heads point at TEV-cleaved TraB₃₁₋₁₁₀. **(C)** CD spectrum of TraB₃₁₋₁₁₀ showing two minima at 209 and 222 nm implying a mainly α -helical conformation of TraB₃₁₋₁₁₀.

anti-TraG antibody showed a band at around 20 kDa, which migrated significantly faster than the calculated MW of 40.4 kDa for TraG. This could mean that only the CHAP domain of TraG is part of the isolated protein complex as the band would correspond to its calculated MW of 22 kDa (Arends et al., 2013).

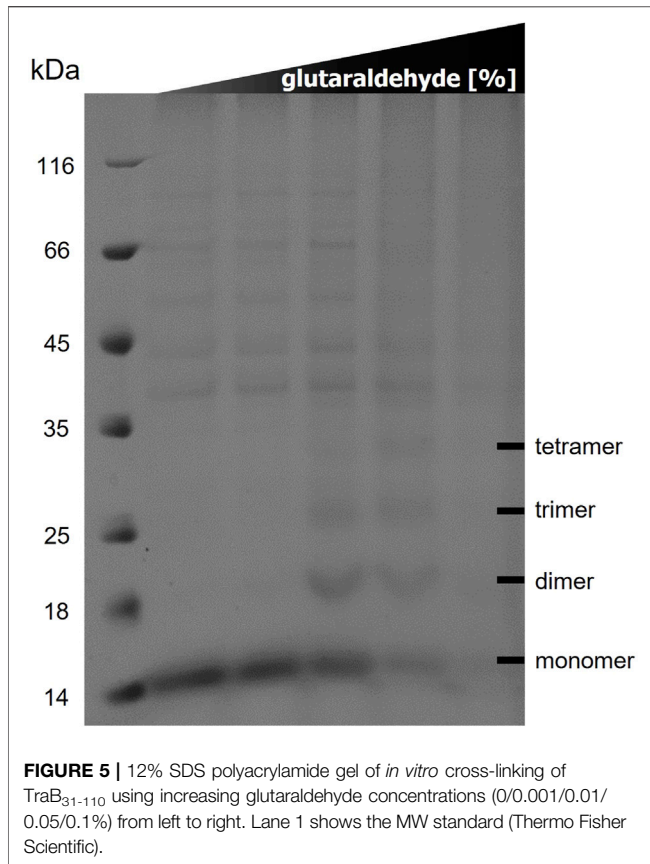
DISCUSSION

In this study, we focused on the small polytopic transmembrane protein TraB. We used biparental matings, pull-down assays and structural analyses to elucidate the potential functional role of TraB in the T4SS_{PIP501}.

TraB was shown to be essential for conjugative pIP501 transfer. Biparental mating assays in *E. faecalis* revealed a total loss of transfer activity for the pIP501 *traB* knockout. The TraB N-terminal signal secretion sequence is crucial for transfer and

location of TraB in the cell envelope. Cell fractionation of *E. faecalis* JH2-2 harboring pIP501, and *E. faecalis* JH2-2 pIP501 Δ *traB*, pEU327-RBS-*traB*-Strep showed its localization in the cell wall and cell membrane fraction (**Figure 2** panel C). However, some residual transfer activity (mean transfer frequency of 1.53×10^{-7} transconjugants/recipient) was detected when only TraB₃₁₋₁₁₀ was present. This residual transfer frequency could possibly result from an association of TraB with TraM or TraG, which could recruit TraB to the membrane *via* protein-protein interaction, as demonstrated in the pull-downs by co-elution of TraM and TraG. In addition, yeast two-hybrid studies suggested an interaction of TraB with TraG (Abajy et al., 2007).

Through pull-down assays, we confirmed the hypothesis that TraB is part of the MPF_{PIP501} complex. It could even act as one of the recruitment factors of the T4SS complex, likely together with the VirB8-like TraM protein and TraG, whose N-terminal TMH

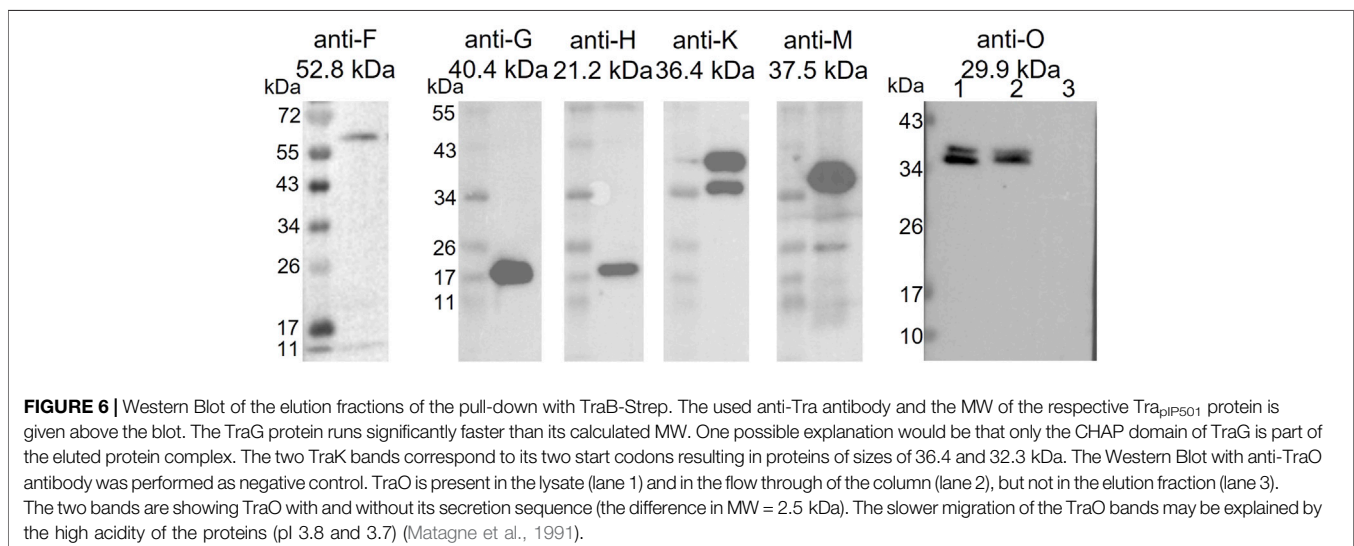


was shown to be required for correct membrane localization of TraM (Kohler et al., 2017). Due to inherent differences between the cell envelopes of Gram+ and Gram- bacteria, *B. megaterium* MS941 was used as an expression host. The strain does not express the major extracellular protease NprM in addition to its inherent alkaline protease deficiency (Wittchen and Meinhardt, 1995), making it a suitable host for the expression of native

T4SS_{PIP501} proteins allowing a proper assembly of the MPF complex. The expression plasmid pMGBm19 harbors the PIP501 *tra* operon from *traB* to *traO* lacking the *traA* gene encoding the relaxase as conjugative relaxases are not involved in the MPF complex (Lang et al., 2010). TraA is essential for DNA transfer as it forms the single-stranded plasmid DNA to be transferred to the recipient, but the number of MPF complexes might be decreased in the presence of TraA as it controls gene expression of the *tra* operon by binding to *oriT* partially overlapping with the main *tra* operon promoter P_{tra} .

TraF, TraH, TraK, TraM, and TraG were shown to coelute with TraB in the pull-downs. The VirB8 homologs TraM and TraH have been proposed as members of the T4SS core complex (Fercher et al., 2016; Kohler et al., 2017; Kohler et al., 2018b). TraF is a structural homolog of a T7SS component (A. Stallinger and W. Keller, personal communication) and together with TraC, TraI and VirB6-like TraL it is likely involved in T4SS complex formation (Abajy et al., 2007; Fercher et al., 2016). The cell envelope-located TraK is also a likely integral component of the core complex (Goessweiner-Mohr et al., 2014b). The lytic transglycosylase TraG was found to be crucial for the T4SS assembly but it is likely not present in the MPF complex itself as proposed in Arends et al. and Kohler et al. (Arends et al., 2013; Kohler et al., 2017). Interestingly, by probing the eluate of the TraB-Strep pull-down with the anti-TraG antibody, we found a protein whose size would fit the MW of the C-terminal domain of TraG, the CHAP domain. The appearance of a protein of the approximate size of the CHAP domain in the eluate is intriguing. We speculate that a hitherto uncharacterized intracellular peptidase in *B. megaterium* might have cleaved the flexible linker region between the SLT and CHAP domain in TraG (Arends et al., 2013; Jeong et al., 2018). Thus, we cannot exclude TraG being a member of the T4SS complex, although the interaction of TraG with the members of the T4SS complex could be only transient.

In addition, in a pull-down performed with TraK-Strep, the same proteins were coeluted, as here demonstrated for the TraB-Strep based pull-down, namely TraF, TraG, TraH, and TraM (data not shown). These data are consistent with the results presented in this study.



For all orthologs of TraB_{pIP501} a similar domain structure and topology was predicted. All orthologs feature a secretion signal sequence, which is cleaved upon secretion, resulting in a mature two-helix transmembrane protein. The most conserved regions were parts of the TMH and the short cytoplasmic loop connecting TMH-1 and TMH-2 (Ditty and Harwood, 1999).

In addition, we created a phylogenetic tree using MEGA version 11 (Tamura et al., 2021) using a higher number of orthologs, including several CagC family proteins. As CagC was proposed to be the major pilin of the *Helicobacter pylori* T4SS, we included two prominent pilin proteins, VirB2 of *Agrobacterium tumefaciens* and *Brucella suis*. The results are shown in **Supplementary Figure S1** and suggest that there is no relevant relation between TraB_{pIP501} and the two pilins. Nevertheless, we aligned their theoretical structure with the theoretical structure of TraB_{pIP501} and show this superposition in **Supplementary Figure S2**. In spite of the topological similarity of their mature forms (two antiparallel α -helices connected by a short loop) the superposition shows a pronounced structural difference and results in a high RMSD deviation. A prominent feature, the kink in the C-terminal α -helix, is common to all presented orthologs, but is missing in the theoretical pilin structures.

The alignment of the theoretical 3D structures of the TraB orthologs in **Figure 3** shows a high structural conservation for TMH-1 and TMH-2 among all orthologs. The highest differences were found in the orientation and length of the first helix, and in the conformation of the flexible linker, which is also part of the secretion signal sequence.

The conserved features of all TraB orthologs such as the length and anti-parallel arrangement of the TMHs, the kink in TMH-2, the tight loop between TMH-1 and TMH-2 and the structurally conserved position of charged and aromatic residues suggest that TraB_{pIP501} and its orthologs play an important role in the formation of the MPF complex. As TraB_{pIP501} is the only protein encoded by the pIP501 *tra* operon (except for TraO that is not part of the MPF), which features a secretion signal sequence, one role of TraB could be that of a recruitment factor for some of the other Tra proteins, which may not be able to self-insert into the membrane. The drastically reduced transfer rate when using TraB₃₁₋₁₁₀ instead of wild type TraB also corroborates its role as a putative recruitment factor. Based on the length and arrangement of the TMHs TraB is also likely to adopt a structural role in building up the MPF complex: the length is consistent with the proposed thickness of the bacterial membrane and the conserved positively charged and aromatic residues are ideally positioned for anchoring the protein in the membrane. As we showed in the *in vitro* cross-link, TraB can form defined oligomers in detergent micelles. The highest oligomerization was found to be a tetramer; however, this might be due to the restriction in size of the protein-micelle complex. In the context of the MPF complex it is well conceivable that TraB forms higher oligomers by self-interaction and possible interactions with other members of the pIP501 T4SS.

Interestingly, TraB orthologs were found on a variety of bacterial species belonging to the phylum Firmicutes. They include putative T4SSs from environmental strains, such as *C. algariphilum* which was first isolated from water brine in permafrost (Shcherbakova et al., 2005) as well as conjugative plasmids from severe nosocomial pathogens such as *S. aureus*, MRSA and *E. faecalis*. pRE25 and

pAM β 1 are, like pIP501, broad-host-range multiresistance plasmids of the inc18 incompatibility group which can transfer virtually to all Gram + bacteria (Kohler et al., 2018b). pV030-8, which was isolated from *S. aureus*, belongs to the pSK41/pGO1 family of multiresistance plasmids capable of promoting conjugative resistance transfer among staphylococci (Firth and Skurray, 2006; Pérez-Roth et al., 2010). The presence of TraB orthologs on T4SSs from a variety of bacterial genera including environmental, biotechnologically relevant as well as pathogenic species points to a crucial role of this small transmembrane protein in the horizontal dissemination of diverse factors including antibiotic resistance genes.

DATA AVAILABILITY STATEMENT

The original contributions presented in the study are included in the article/**Supplementary Material**, further inquiries can be directed to the corresponding authors.

AUTHOR CONTRIBUTIONS

Conceptualization, CM, EG, TB, and WK; methodology, BG, CM, EG, IP, LP, SP, TB, TP-K, TS, and WK; investigation, BG, CM, EG, IP, LP, SP, TB, TP-K, TS, and WK; resources, EG, TP-K, and WK; writing original draft preparation, CM, EG, TB, and WK; writing, review and editing, BG, CM, EG, IP, TB, TP-K, and WK; supervision, EG, TP-K, and WK; funding acquisition, EG and TP-K. All authors have read and agreed to the published version of the manuscript.

FUNDING

Financial support of the Doctoral Academy, Consortium Doc. Funds BioMolStruct (DOC130), University of Graz, is highly acknowledged. This research was funded in part by grants from the Austrian Science Fund (FWF), Grant numbers: DOC130 and SFB F4604. The Berliner Hochschule für Technik, Berlin, Germany, funded the doctoral thesis of CM. The authors acknowledge the financial support for open access publication by the University of Graz.

ACKNOWLEDGMENTS

We thank Verena Kohler and Kristin Hunger for construction of pMGBm19-RBS-*traB-traO* and David Glück for assistance in preparation and analysis of the MS samples. MS-Proteomics was supported by the Field of Excellence BioHealth - University of Graz.

SUPPLEMENTARY MATERIAL

The Supplementary Material for this article can be found online at: <https://www.frontiersin.org/articles/10.3389/fmolb.2022.867136/full#supplementary-material>

REFERENCES

- Abajy, M. Y., Kopec', J., Schiwon, K., Burzynski, M., Döring, M., Bohn, C., et al. (2007). A Type IV-secretion-like System Is Required for Conjugative DNA Transport of Broad-Host-Range Plasmid pIP501 in Gram-Positive Bacteria. *J. Bacteriol.* 189, 2487–2496. doi:10.1128/JB.01491-06
- Almagro Armenteros, J. J., Tsirigos, K. D., Sønderby, C. K., Petersen, T. N., Winther, O., Brunak, S., et al. (2019). Signalp 5.0 Improves Signal Peptide Predictions Using Deep Neural Networks. *Nat. Biotechnol.* 37, 420–423. doi:10.1038/s41587-019-0036-z
- Alvarez-Martinez, C. E., and Christie, P. J. (2009). Biological Diversity of Prokaryotic Type IV Secretion Systems. *Microbiol. Mol. Biol. Rev.* 73, 775–808. doi:10.1128/MMBR.00023-09
- Arends, K., Celik, E.-K., Probst, I., Goessweiner-Mohr, N., Fercher, C., Grumet, L., et al. (2013). TraG Encoded by the pIP501 Type IV Secretion System Is a Two-Domain Peptidoglycan-Degrading Enzyme Essential for Conjugative Transfer. *J. Bacteriol.* 195, 4436–4444. doi:10.1128/JB.02263-12
- Baek, M., DiMaio, F., Anishchenko, I., Dauparas, J., Ovchinnikov, S., Lee, G. R., et al. (2021). Accurate Prediction of Protein Structures and Interactions Using a Three-Track Neural Network. *Science* 373, 871–876. doi:10.1126/SCIENCE.ABJ8754
- Biedendieck, R., Borgmeier, C., Bunk, B., Stammen, S., Scherling, C., Meinhardt, F., et al. (2011). Systems Biology of Recombinant Protein Production Using *Bacillus Megaterium*. *Methods Enzymol.* 500, 165–195. doi:10.1016/B978-0-12-385118-5.00010-4
- Bryson, K., Cozzetto, D., and Jones, D. (2007). Computer-Assisted Protein Domain Boundary Prediction Using the Dom-Pred Server. *Cpps* 8, 181–188. doi:10.2174/138920307780363415
- Buchan, D. W. A., and Jones, D. T. (2019). The PSIPRED Protein Analysis Workbench: 20 Years on. *Nucleic Acids Res.* 47, W402–W407. doi:10.1093/NAR/GKZ297
- Chang, J.-M., Di Tommaso, P., and Notredame, C. (2014). TCS: a New Multiple Sequence Alignment Reliability Measure to Estimate Alignment Accuracy and Improve Phylogenetic Tree Reconstruction. *Mol. Biol. Evol.* 31, 1625–1637. doi:10.1093/molbev/msu117
- Chang, J.-M., Di Tommaso, P., Taly, J.-F., and Notredame, C. (2012). Accurate Multiple Sequence Alignment of Transmembrane Proteins with PSI-Coffee. *BMC Bioinformatics* 13 (Suppl. 4), S1. doi:10.1186/1471-2105-13-S4-S1
- Chang, J.-M., Di Tommaso, P., Lefort, V., Gascuel, O., and Notredame, C. (2015). TCS: a Web Server for Multiple Sequence Alignment Evaluation and Phylogenetic Reconstruction: Figure 1. *Nucleic Acids Res.* 43, W3–W6. doi:10.1093/nar/gkv310
- Christie, P. J. (2016). The Mosaic Type IV Secretion Systems. *EcoSal Plus* 7, 1–34. doi:10.1128/ecosalplus.ESP-0020-2015
- Compton, L. A., and Johnson, W. C. (1986). Analysis of Protein Circular Dichroism Spectra for Secondary Structure Using a Simple Matrix Multiplication. *Anal. Biochem.* 155, 155–167. doi:10.1016/0003-2697(86)90241-1
- Costa, T. R. D., Harb, L., Khara, P., Zeng, L., Hu, B., and Christie, P. J. (2021). Type IV Secretion Systems: Advances in Structure, Function, and Activation. *Mol. Microbiol.* 115, 436–452. doi:10.1111/mmi.14670
- Cox, J., and Mann, M. (2008). MaxQuant Enables High Peptide Identification Rates, Individualized p.p.b.-range Mass Accuracies and Proteome-wide Protein Quantification. *Nat. Biotechnol.* 26, 1367–1372. doi:10.1038/nbt.1511
- de Planque, M. R. R., Kruijtzter, J. A. W., Liskamp, R. M. J., Marsh, D., Greathouse, D. V., Koeppel, R. E., et al. (1999). Different Membrane Anchoring Positions of Tryptophan and Lysine in Synthetic Transmembrane α -Helical Peptides. *J. Biol. Chem.* 274, 20839–20846. doi:10.1074/jbc.274.30.20839
- Ditty, J. L., and Harwood, C. S. (1999). Conserved Cytoplasmic Loops Are Important for Both the Transport and Chemotaxis Functions of PcaK, a Protein from *Pseudomonas Putida* with 12 Membrane-Spanning Regions. *J. Bacteriol.* 181, 5068–5074. doi:10.1128/JB.181.16.5068-5074.1999
- Fercher, C., Probst, I., Kohler, V., Goessweiner-Mohr, N., Arends, K., Grohmann, E., et al. (2016). VirB8-like Protein TraH Is Crucial for DNA Transfer in *Enterococcus faecalis*. *Sci. Rep.* 6, 24643. doi:10.1038/srep24643
- Firth, N., and Skurray, R. A. (2006). “Genetics: Accessory Elements and Genetic Exchange,” in *Gram-Positive Pathogens*. Editors V. A. Fischetti, R. P. Novick, J. J. Ferretti, D. A. Portnoy, and J. I. Rood (Washington, DC, USA: ASM Press), 413–426.
- Fischer, W., Tegtmeyer, N., Stingl, K., and Backert, S. (2020). Four Chromosomal Type IV Secretion Systems in *Helicobacter pylori*: Composition, Structure and Function. *Front. Microbiol.* 11, 1592. doi:10.3389/fmicb.2020.01592
- García-Solache, M., and Rice, L. B. (2019). The *Enterococcus*: a Model of Adaptability to its Environment. *Clin. Microbiol. Rev.* 32. doi:10.1128/CMR.00058-18
- Gasteiger, E., Hoogland, C., Gattiker, A., Duvaud, S. e., Wilkins, M. R., Appel, R. D., et al. (2005). “Protein Identification and Analysis Tools on the ExPASy Server,” in *The Proteomics Protocols Handbook*. Editor J. M. Walker (Totowa, NJ: Humana Press), 571–607. doi:10.1385/1-59259-890-0:571
- Gesslbauer, B., Kuerzl, D., Valpatic, N., and Bochkov, V. (2018). Unbiased Identification of Proteins Covalently Modified by Complex Mixtures of Peroxidized Lipids Using a Combination of Electrophoretic Mobility Band Shift with Mass Spectrometry. *Antioxidants* 7, 116. doi:10.3390/antiox7090116
- Goessweiner-Mohr, N., Arends, K., Keller, W., and Grohmann, E. (2014a). Conjugation in Gram-Positive Bacteria. *Microbiol. Spectr.* 2, PLAS-0004-2013. doi:10.1128/microbiolspec.PLAS-0004-2013
- Goessweiner-Mohr, N., Fercher, C., Arends, K., Birner-Gruenberger, R., Laverde-Gomez, D., Huebner, J., et al. (2014b). The Type IV Secretion Protein TraK from the *Enterococcus* conjugative Plasmid pIP501 Exhibits a Novel Fold. *Acta Cryst. D Biol. Crystallogr.* 70, 1124–1135. doi:10.1107/S1399004714001606
- Goessweiner-Mohr, N., Grumet, L., Arends, K., Pavkov-Keller, T., Gruber, C. C., Gruber, K., et al. (2013). The 2.5 Å Structure of the Enterococcus Conjugation Protein TraM Resembles VirB8 Type IV Secretion Proteins. *J. Biol. Chem.* 288, 2018–2028. doi:10.1074/jbc.M112.428847
- Grohmann, E., Christie, P. J., Waksman, G., and Backert, S. (2018). Type IV Secretion in Gram-Negative and Gram-Positive Bacteria. *Mol. Microbiol.* 107, 455–471. doi:10.1111/mmi.13896
- Grohmann, E., Goessweiner-Mohr, N., and Brantl, S. (2016). DNA-binding Proteins Regulating pIP501 Transfer and Replication. *Front. Mol. Biosci.* 3, 42. doi:10.3389/fmolb.2016.00042
- Grohmann, E., Keller, W., and Muth, G. (2017). Mechanisms of Conjugative Transfer and Type IV Secretion-Mediated Effector Transport in Gram-Positive Bacteria. *Curr. Top. Microbiol. Immunol.* 413, 115–141. doi:10.1007/978-3-319-75241-9_5
- Grohmann, E., Muth, G., and Espinosa, M. (2003). Conjugative Plasmid Transfer in Gram-Positive Bacteria. *Microbiol. Mol. Biol. Rev.* 67, 277–301. table of contents. doi:10.1128/MMBR.67.2.277-301.2003
- Horodniceanu, T., Bouanchaud, D. H., Bieth, G., and Chabbert, Y. A. (1976). R Plasmids in *Streptococcus Agalactiae* (Group B). *Antimicrob. Agents Chemother.* 10, 795–801. doi:10.1128/aac.10.5.795
- Jeong, Y. J., Baek, S. C., and Kim, H. (2018). Cloning and Characterization of a Novel Intracellular Serine Protease (IspK) from *Bacillus Megaterium* with a Potential Additive for Detergents. *Int. J. Biol. Macromolecules* 108, 808–816. doi:10.1016/j.ijbiomac.2017.10.173
- Kim, M., Park, J., Kang, M., Yang, J., and Park, W. (2021). Gain and Loss of Antibiotic Resistant Genes in Multidrug Resistant Bacteria: One Health Perspective. *J. Microbiol.* 59, 535–545. doi:10.1007/s12275-021-1085-9
- Kohler, V., Goessweiner-Mohr, N., Aufschneider, A., Fercher, C., Probst, I., Pavkov-Keller, T., et al. (2018a). TraN: A Novel Repressor of an *Enterococcus* Conjugative Type IV Secretion System. *Nucleic Acids Res.* 46, 9201–9219. doi:10.1093/nar/gky671
- Kohler, V., Probst, I., Aufschneider, A., Büttner, S., Schaden, L., Rechberger, G. N., et al. (2017). Conjugative Type IV Secretion in Gram-Positive Pathogens: TraG, a Lytic Transglycosylase and Endopeptidase, Interacts with Translocation Channel Protein TraM. *Plasmid* 91, 9–18. doi:10.1016/j.plasmid.2017.02.002
- Kohler, V., Vaishampayan, A., and Grohmann, E. (2018b). Broad-host-range Inc18 Plasmids: Occurrence, Spread and Transfer Mechanisms. *Plasmid* 99, 11–21. doi:10.1016/j.plasmid.2018.06.001
- Krawczyk, B., Wityk, P., Gałęcka, M., and Michalik, M. (2021). The Many Faces of *Enterococcus* spp.-Commensal, Probiotic and Opportunistic Pathogen. *Microorganisms* 9, 1900. doi:10.3390/microorganisms9091900
- Kristich, C. J., Chandler, J. R., and Dunny, G. M. (2007). Development of a Host-genotype-independent Counterselectable Marker and a High-Frequency Conjugative Delivery System and Their Use in Genetic Analysis of

- Enterococcus faecalis*. *Plasmid* 57, 131–144. doi:10.1016/j.plasmid.2006.08.003
- Kurenbach, B., Bohn, C., Prabhu, J., Abudukerim, M., Szewzyk, U., and Grohmann, E. (2003). Intergeneric transfer of the *Enterococcus faecalis* plasmid pIP501 to *Escherichia coli* and *Streptomyces lividans* and sequence analysis of its *tra* region. *Plasmid* 50, 86–93. doi:10.1016/S0147-619X(03)00044-1
- Laemmli, U. K. (1970). Cleavage of Structural Proteins during the Assembly of the Head of Bacteriophage T4. *Nature* 227, 680–685. doi:10.1038/227680a0
- Landolt-Marticorena, C., Williams, K. A., Deber, C. M., and Reithmeier, R. A. F. (1993). Non-random Distribution of Amino Acids in the Transmembrane Segments of Human Type I Single Span Membrane Proteins. *J. Mol. Biol.* 229, 602–608. doi:10.1006/jmbi.1993.1066
- Lang, S., Gruber, K., Mihajlovic, S., Arnold, R., Gruber, C. J., Steinlechner, S., et al. (2010). Molecular Recognition Determinants for Type IV Secretion of Diverse Families of Conjugative Relaxases. *Mol. Microbiol.* 78, 1539–1555. doi:10.1111/j.1365-2958.2010.07423.x
- Levitus, M., Rewane, A., and Perera, T. B. (2022). *Vancomycin-Resistant Enterococci*. Treasure Island (FL): StatPearls Publishing.
- Li, Y. G., and Christie, P. J. (2018). The *Agrobacterium* VirB/VirD4 T4SS: Mechanism and Architecture Defined through *In Vivo* Mutagenesis and Chimeric Systems. *Curr. Top. Microbiol. Immunol.* 418, 233–260. doi:10.1007/82_2018_94
- Lin, Z., Yuan, T., Zhou, L., Cheng, S., Qu, X., Lu, P., et al. (2021). Impact Factors of the Accumulation, Migration and Spread of Antibiotic Resistance in the Environment. *Environ. Geochem. Health* 43, 1741–1758. doi:10.1007/s10653-020-00759-0
- Matagne, A., Joris, B., and Frère, J. M. (1991). Anomalous Behaviour of a Protein during SDS/PAGE Corrected by Chemical Modification of Carboxylic Groups. *Biochem. J.* 280 (Pt 2), 553–556. doi:10.1042/bj2800553
- Meier, F., Brunner, A.-D., Koch, S., Koch, H., Lubeck, M., Krause, M., et al. (2018). Online Parallel Accumulation-Serial Fragmentation (PASEF) with a Novel Trapped Ion Mobility Mass Spectrometer. *Mol. Cell Proteomics* 17, 2534–2545. doi:10.1074/mcp.TIR118.000900
- Miles, A. J., Ramalli, S. G., and Wallace, B. A. (2022). DichroWeb, a Website for Calculating Protein Secondary Structure from Circular Dichroism Spectroscopic Data. *Protein Sci.* 31, 37–46. doi:10.1002/PRO.4153
- Moffat, L., and Jones, D. T. (2021). Increasing the Accuracy of Single Sequence Prediction Methods Using a Deep Semi-supervised Learning Framework. *Bioinformatics* 37, 3744–3751. doi:10.1093/bioinformatics/btab491
- Notredame, C., Higgins, D. G., and Heringa, J. (2000). T-coffee: a Novel Method for Fast and Accurate Multiple Sequence Alignment 1 Edited by J. Thornton. *J. Mol. Biol.* 302, 205–217. doi:10.1006/jmbi.2000.4042
- Nugent, T., and Jones, D. T. (2009). Transmembrane Protein Topology Prediction Using Support Vector Machines. *BMC Bioinformatics* 10, 159. doi:10.1186/1471-2105-10-159
- Nugent, T., Ward, S., and Jones, D. T. (2011). The MEMPACK Alpha-Helical Transmembrane Protein Structure Prediction Server. *Bioinformatics* 27, 1438–1439. doi:10.1093/bioinformatics/btr096
- Ortiz Charneco, G., Kelleher, P., Buivydas, A., Streekstra, H., van Themaat, E. V. L., de Waal, P. P., et al. (2021). Genetic Dissection of a Prevalent Plasmid-Encoded Conjugation System in *Lactococcus lactis*. *Front. Microbiol.* 12, 680920. doi:10.3389/fmicb.2021.680920
- Palmer, K. L., Kos, V. N., and Gilmore, M. S. (2010). Horizontal Gene Transfer and the Genomics of Enterococcal Antibiotic Resistance. *Curr. Opin. Microbiol.* 13, 632–639. doi:10.1016/j.mib.2010.08.004
- Pe' rez-Roth, E., Kwong, S. M., Alcoba-Florez, J., Firth, N., and Me' ndez-A' lvarez, S. (2010). Complete Nucleotide Sequence and Comparative Analysis of pPR9, a 41.7-kilobase Conjugative Staphylococcal Multiresistance Plasmid Conferring High-Level Mupirocin Resistance. *Antimicrob. Agents Chemother.* 54, 2252–2257. doi:10.1128/AAC.01074-09
- Phillips, R. (2018). “Membranes by the Numbers,” in *Physics of Biological Membranes*. Editors P. Bassereau and P. Sens (Cham: Springer International Publishing), 73–105. doi:10.1007/978-3-030-00630-3_3
- Rath, A., Glibowicka, M., Nadeau, V. G., Chen, G., and Deber, C. M. (2009). Detergent Binding Explains Anomalous SDS-PAGE Migration of Membrane Proteins. *Proc. Natl. Acad. Sci. U.S.A.* 106, 1760–1765. doi:10.1073/pnas.0813167106
- Schrödinger, L., and DeLano, W. (2020). *The PyMOL Molecular Graphics System, Version 2.5.2*. New York, NY: Schrödinger, LLC. Retrieved from <http://www.pymol.org/pymol>.
- Shcherbakova, V. A., Chuvilskaya, N. A., Rivkina, E. M., Pecheritsyna, S. A., Laurinavichius, K. S., Suzina, N. E., et al. (2005). Novel Psychrophilic Anaerobic Spore-Forming Bacterium from the Overcooled Water Brine in Permafrost: Description *Clostridium Algoriphilum* Sp. Nov. *Extremophiles* 9, 239–246. doi:10.1007/s00792-005-0438-3
- Shindyalov, I. N., and Bourne, P. E. (1998). Protein Structure Alignment by Incremental Combinatorial Extension (CE) of the Optimal Path. *Protein Eng. Des. Selection* 11, 739–747. doi:10.1093/protein/11.9.739
- Tamura, K., Stecher, G., and Kumar, S. (2021). MEGA11: Molecular Evolutionary Genetics Analysis Version 11. *Mol. Biol. Evol.* 38, 3022–3027. doi:10.1093/molbev/msab120
- Wittchen, K.-D., and Meinhardt, F. (1995). Inactivation of the Major Extracellular Protease from *Bacillus Megaterium* DSM319 by Gene Replacement. *Appl. Microbiol. Biotechnol.* 42, 871–877. doi:10.1007/BF00191184

Conflict of Interest: The authors declare that the research was conducted in the absence of any commercial or financial relationships that could be construed as a potential conflict of interest.

Publisher's Note: All claims expressed in this article are solely those of the authors and do not necessarily represent those of their affiliated organizations, or those of the publisher, the editors and the reviewers. Any product that may be evaluated in this article, or claim that may be made by its manufacturer, is not guaranteed or endorsed by the publisher.

Copyright © 2022 Berger, Michaelis, Probst, Sagmeister, Petrowitsch, Puchner, Pavkov-Keller, Gesslbauer, Grohmann and Keller. This is an open-access article distributed under the terms of the Creative Commons Attribution License (CC BY). The use, distribution or reproduction in other forums is permitted, provided the original author(s) and the copyright owner(s) are credited and that the original publication in this journal is cited, in accordance with accepted academic practice. No use, distribution or reproduction is permitted which does not comply with these terms.